Int J Clin Exp Med 2015;8(6):9192-9204
www.ijcem.com /ISSN:1940-5901/IJCEM0008866

Original Article

Mitochondrial and cytoskeletal alterations are involved in the pathogenesis of hydronephrosis in ICR/Mlac-*hydro* mice

Duangnate Isarangkul[1], Suthep Wiyakrutta[1], Kanchana Kengkoom[2], Onrapak Reamtong[3], Sumate Ampawong[4]

[1]Department of Microbiology, Faculty of Science, Mahidol University, 272, Rama VI Road, Ratchathewi, Bangkok 10400, Thailand; [2]Office of Academic Services, National Laboratory Animal Center, Mahidol University, 999, Phutthamonthon 4 Road, Salaya, Phutthamonthon, Nakhon Pathom 73170, Thailand; Departments of [3]Molecular Tropical Medicine and Genetic, [4]Tropical Pathology, Faculty of Tropical Medicine, Mahidol University, 420/6, Ratchawithi Road, Ratchathewi, Bangkok 10400, Thailand

Received April 8, 2015; Accepted June 7, 2015; Epub June 15, 2015; Published June 30, 2015

Abstract: The pathogenesis of congenital hydronephrosis in laboratory animals has been studied for many years, yet little is known about the underlying mechanism of this disease. In this study, we investigated a MS-based comparative proteomics approach to characterize the differently expressed proteins between kidney tissue samples of ICR/Mlac-*hydro* and wild-type mice. Interestingly, proteomic results exhibited several mitochondrial protein alterations especially the up-regulation of 60 kDa heat shock protein (Hsp60), stress-70 protein (GRP75) dysfunction, and down-regulation of voltage-dependent anion-selective channel protein 1 (VDAC-1). The results demonstrated that mitochondrial alteration may lead to inadequate energy-supply to maintain normal water reabsorption from the renal tubule, causing hydronephrosis. Moreover, the alteration of cytoskeleton proteins in the renal tubule, in particular the up-regulation of tubulin beta-4B chain (Tb4B) and N-myc downstream-regulated gene 1 protein (Ndr-1) may also be related due to their fundamental roles in maintaining cell morphology and tissue stability. In addition, cytoskeletal alterations may consequence to the reduction of glyceraldehydes-3-phosphate dehydrogenase (GAPDH), cytoplasmic enzyme, which modulates the capacity of structural proteins. Our findings highlight a number of target proteins that may play a crucial role in congenital hydronephrosis and emphasize that the disorder of mitochondria and cytoskeleton proteins may be involved.

Keywords: Cytoskeleton, hydronephrosis, ICR/Mlac-*hydro* mice, mitochondria, pathogenesis, proteomic

Introduction

Hydronephrosis refers to the distension and dilatation of the renal pelvis and calyces, with accompanying atrophy to the parenchyma, caused by obstructed of urine outflow [1]. This obstruction may present itself mechanically [1, 2] and functionally [3]. Congenital hydronephrosis still remains a priority of antenatal detected urinary tract abnormalities in mankind. More importantly, congenital hydronephrosis is one of five major birth defects subordinated to atrial septal defect and ventricular septal defect with accumulated incidence of 15-580 cases per 10,000 newborns [4-6]. To understand the pathophysiology of congenital hydronephrosis better, several spontaneously-arising animal models, (STR/N mouse, NZC mouse, C3H mouse, BRVR mouse, C57BL/KsJ mouse, C57L/MsNrs mouse, DDD inbred mouse, and *cph/cph* mouse) have been developed as the study model for urinary tract diseases in biomedical research [3, 7-13].

The ICR/Mlac-*hydro* mice were established by selective inbreeding of ICR mice carrying the hydronephrosis mutation [14]. Our recent studies demonstrated that the mice develop bilateral non-obstructive hydronephrosis without evidence of interstitial fibrosis and glomerulosclerosis [15]. They also display no abnormalities in blood urea nitrogen, creatinine concentration, and urine-specific gravity. Interestingly, these mice exhibit trabeculae bone loss, possibly caused by marked decreases in both osteoblast and osteoclast activities [16]. Since

chronic renal disease stage affects to bone formation. However the pathogenic roles of this hydronephrotic model have not yet been studied.

Proteomics is the large-scale analysis of proteins in biological mixtures, and provides evidence for protein expression levels regard to molecular mechanisms, underlying health, diseases, and pinpoints potential disease biomarkers [17]. There are many associated potential protein markers for renal diseases such as nephrin and podocin for glomerular injury in diabetic nephropathy [18], podocalyxin for glomerular injury in lupus nephritis [19], NGAL, KIM-1, and NAG for tubulointerstitial injury in acute and chronic kidney diseases [20], and proSAAS in newborn obstructive nephropathy [21]. Recent comparative proteomic analysis suggests that mitochondria are involved in autosomal recessive polycystic kidney disease [22].

Along this line of though, in this study, we conducted proteomics approach to explore the protein expression profile of renal tissues from ICR/Mlac-*hydro* and wild-type mice to identify which proteins are involved in or control the characteristics of hydronephrosis. To confirm the proteomics results, further analysis was detected by immunohistochemical study. It is expected that the results of this study provide new insights into the understanding of the pathogenesis underlying congenital hydronephrosis and preliminary guideline for therapeutic approach.

Materials and methods

Ethics statement

Animal studies were performed in accordance with the Mahidol University policy for the care and use of animals for scientific purposes and approved by the institutional ethic committee (Animal Welfare Assurance Number: RA2007-01.01). Sixty days old of five male ICR/Mlac-*hydro* mice (hydronephrosis strain) and five male wild-type mice (free hydronephrosis strain) from National Laboratory Animal Center, Mahidol University were included in the study.

Sample preparation

Blood samples from each group were collected by cardiac puncture under anesthesia with carbon dioxide inhalation and the mice were humanely sacrificed by exsanguination. Creatinine and blood urea nitrogen (BUN) were measured by a Hitachi 902 automated blood analyzer (Hitachi Science Systems Ltd., Ibaraki, Japan). A necropsy examination was performed on each animal with grossly examined study of the urinary tract. Urine from the urinary bladder was collected into a clean syringe for spectroscopic measurement of urine specific gravity. The kidneys were given cranial-longitudinal incisions, one half was fixed in 10% neutral buffered formalin for histological and immunohistochemical studies and the other was snap frozen in liquid nitrogen then stored in -70 to -80°C for proteomic analysis. Fixed specimens were routinely processed, embedded in paraffin, 5-μm sectioned, and stained with hematoxylin & eosin (H&E).

Histomorphology

The degree of hydronephrosis was determined by measuring the percentage of renal parenchyma as assessed by an imaging analysis program (ImageJ® Version 1.36; National Institutes of Health; Bethesda, Maryland, USA). Briefly, a line was drawn on the overall area of the kidney and the remaining parenchymal area, and then these areas were measured in μm^2. Percentage of renal parenchyma was calculated by extrapolation.

2DE

2DE was modified from a previous study [22]. Snap frozen specimens of renal tissue samples in both ICR/Mlac-*hydro* (n = 3) and wild-type mice (n = 3) were homogenized in liquid nitrogen, and 100 mg of renal tissue was lysed in 500 μl of lysis buffer (7 M urea, 2 M thiourea, 4% CHAPS; Bio-Rad®) containing 1% (v/v) protease inhibitor (Sigma®). Samples were lysed by ultrasonication in an ice bath for eight cycles, each comprising of a 5-s sonication followed by a 10-s break, and then held for 30 min on ice with periodic vortex. After centrifugation at 12,000×*g* for 20 min at 4°C, the supernatant was precipitated with cold acetone (1:4) overnight at -20°C. Next, sample were centrifuged at 14,000×*g* for 15 min at 4°C, pellets were dissolved with 500 μl of rehydration buffer (7 M urea, 2 M thiourea, 4% CHAPS, 120 mM DTT, 2% IPG buffer, 0.002% bromophenol blue). Protein sample concentrations were determined by protein assay reagent (Bio-Rad®)

using a spectrophotometer (NanoDrop-1000, Thermo Scientific). Protein samples (200 µg) in rehydration buffer (total volume = 250 µl) were applied to Immobiline™ Drystrip IPG strip (13 cm, pH 3-10 NL, GE healthcare®) using a passive rehydration method for 12 h. Isoelectric focusing was performed at 20°C using Ettan IPGphor (GE healthcare®) as follows: 500 V (step and hold) for 3 h, 1,000 V (Gradient) for 1 h, 8,000 V (Gradient) for 2.5 h, and finally 8,000 V (step and hold) for 45 min. Following the IEF separation, the gel strips were incubated with gentle shaking in an equilibration solution I (75 mM Tris-HCl, pH 8.8, 6 M urea, 30% glycerol, 2% SDS, 0.002% bromophenol blue, 1.0% DTT) for 15 min, then the strips were again put in an equilibration solution II (75 mM Tris-HCl, pH 8.8, 6 M urea, 30% glycerol, 2% SDS, 0.002% bromophenol blue, 2.5% iodoacetamide) for 15 min. The equilibrated gel strips were placed on the top of a 12.5% SDS-PAGE (2^{nd} dimension) slab gels and sealed with agarose sealing solution (25 mM Tris base, 192 mM glycine, 0.1% SDS, 0.5% agarose, 0.002% bromophenol blue). SDS-PAGE was performed for 30 min at a constant current of 15 mA/gel, and then at 30 mA/gel using a vertical slab gel electrophoresis unit (SE 600 Chroma Hoefer®) until the bromophenol blue reached the bottom of the gels. Immediately after the 2nd dimension run, gels were fixed for 2 h in 40% ethanol containing 10% acetic acid. The gels were then stained with Flamingo™ Fluorescent gel stain (Bio-Rad®) for 18 h on a rocking shaker. Excess dye was washed out from the gel with distilled water. The 2DE was performed on each kidney individually, and the experiments were replicated three times.

Image analysis

The gels were scanned with the Typhoon Trio Variable Mode Imager (GE Healthcare®) at Green laser (532 nm) and 555 nm long pass emission filter. Spot detection, quantification, and comparison of 2D protein patterns were done with the Image Master 2D software (GE healthcare®). The quantity of each spot in a gel was normalized as a percentage of the total quantity in the map according to its OD value. Significant spots were identified as the difference in per cent volume between the groups by ANOVA p-value < 0.05. 20 significant spots were selected for protein identification.

In-gel tryptic digestion

Gel digestion was conducted as previously described [23]. The selected protein spots were manually excised with sterilized pipette tips and dehydrated in acetonitrile (HPLC grade, Merk®). In-gel reduction and alkylation were performed by incubating the gel pieces in DTT solution (10 mM DTT in 100 mM NH_4HCO_3) for 1 h, at 56°C, and then in iodoacetamide (55 mM iodoacetamide in 100 mM NH_4HCO_3) for 45 min, at room temperature with light protection. The gel pieces were then washed with 100 mM NH_4HCO_3, before being pre-incubated in 25-35 µl of trypsin digestive buffer (12.5 ng/µl sequencing grade modified trypsin (Promega) in 50 mM NH_4HCO_3) for 45 min, at 4°C. The redundant trypsin solution was removed and submerged in 5-10 µl of 50 mM NH_4HCO_3 buffer to completely immerse the gel pieces, which were incubated overnight at 37°C (14-16 h). Tryptic digests were extracted with 20 mM NH_4HCO_3 buffer followed by double extraction with 5% formic acid in 50% acetonitrile for 20 min, at room temperature. At the time of extraction, samples were centrifuged at 14,000×*g* for 1 min, then the supernatant was collected. The extracts were dried in a SpeedVac concentrator (Thermo Scientific) at room temperature and then subjected to MS.

MS/MS analysis and protein identification

Mass spectra were examined externally by Salaya Central Instrument Facility (SCIF), Mahidol University using a Nano LC/MS/MS, Maxis UHR-QTOF (Bruker) coupled to a Nano LC System (Dionex). The LC-MS/MS data files were converted into the mascot generic file (.mgf) using DataAnalysisTM software, version 3.4. The mgf files were searched using Mascot version 2.4.1 (Matrix Science, London, UK) against the SwissProt database.

Immunohistochemistry

From the MS/MS analysis and protein identification results, two significantly increased protein markers in the mutant mice were further analyzed by immunohistochemical staining, polyclonal rabbit anti 60 kDa heat shock protein (Hsp60) (Bioss, USA, 900291W) and polyclonal rabbit anti tubulin beta-4B chain (Tb4B) (Bioss, USA, 9H20Y1). Four micron thick sections from the paraffin blocks were cut and

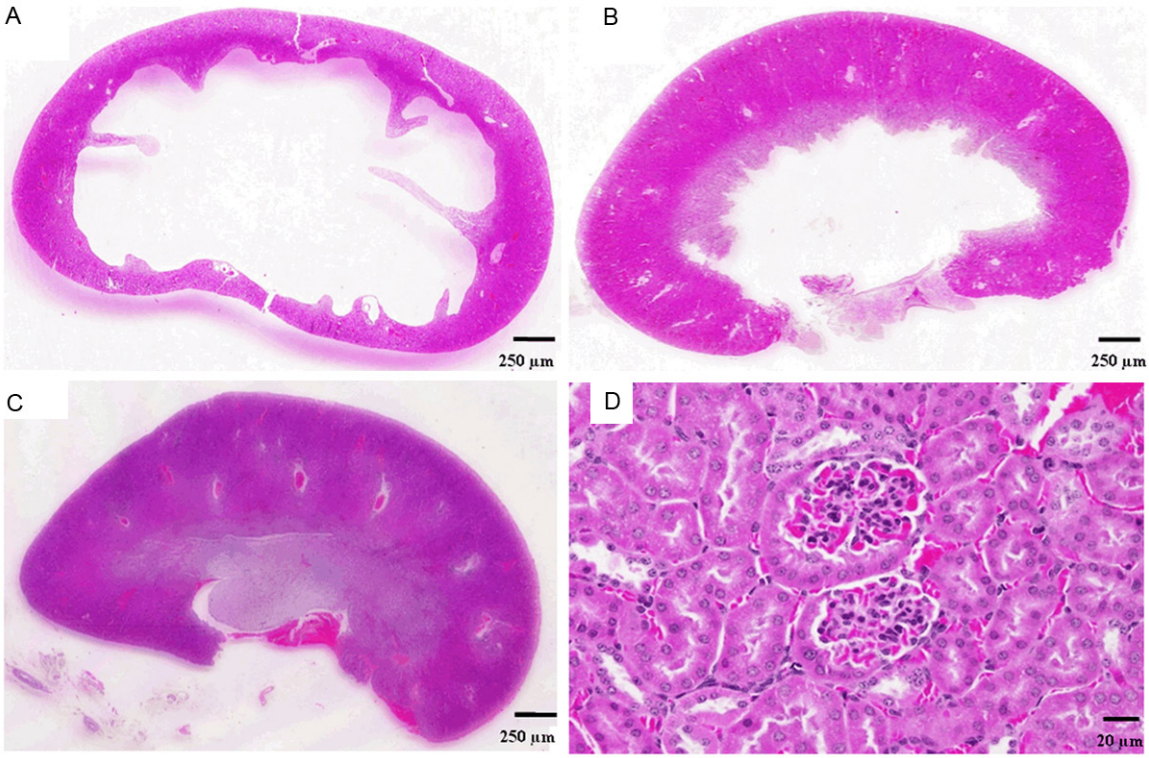

Figure 1. Histopathology of kidney from wild type and ICR/Mlac-*hydro* (H&E staining). (A, B) 60 days old male ICR/Mlac-*hydro* mouse kidney characterized parenchymal atrophy and expansion of pelvicocaliceal space when compared to control mouse (C). (D) Glomerular and tubular architecture were preserved in ICR/Mlac-*hydro* mouse.

Table 1. Comparison of renal parenchyma (%) of ICR/Mlac-*hydro* and wild-type mice

Age (Day)	Sex	Side	% Renal parenchyma (Mean ± SD)		*p*-value
			ICR/Mlac-*hydro*	Wild type	
60	M	Left	59.57 ± 9.7	91.67 ± 4.5	.000
		Right	47.45 ± 10.4	92.67 ± 3.8	.000

placed on pre-coated immunohistochemistry slides, and dried overnight at 56°C then allowed to cool. The sections were deparaffinized in xylene and rehydrated prior to immunostaining. Heat-induced antigen retrieval with citrate buffer (pH 6) was used to unmask the antigen from all antibodies. Endogenous peroxidase was quenched with 3% v/v hydrogen peroxide in methanol after sections were cooled. The sections were washed with 0.2% v/v Tween in Phosphate buffered saline (PBS) and blocked with protein block serum free (Dako, Denmark, X0909) for 10 min. Sections were incubated in primary antibody diluted in PBS with 1% v/v normal goat serum (NGS, Vector, USA, S1000). The sections were washed and incubated for 30 min with labeled polymer HRP anti-mouse/rabbit EnVision kit (Dako, Denmark, K5007) at room temperature, and visualized with diaminobenzidine (DAB, Dako, Denmark, K3468). The slides were counterstained with hematoxylin before permanent mounting with Permount®.

In each group, ten random fields at 400 magnifications were examined by collecting duct and distal tubule. Color images (640 × 480 pixel resolution) were obtained with a light microscope (BX51, Olympus®) and digital camera (DP70, Olympus®). Immunohistochemical expression was then analyzed by a semi-quantitative digitalized image analysis program using ImageJ [24]. Briefly, color images were first converted to 8 bit format in gray scale. Adjusted images were transformed by threshold mode to locate the area of expression. Then, the area of positive reaction was estimated by the number of black pixels determining the percentage of black pixels/high power field.

Statistics

All experimental data were presented as means ± SD and analyzed by independent t-test and one way ANOVA test using IBM® SPSS® statisti-

Table 2. Clinical chemistry (BUN and creatinine) and urine specific gravity of ICR/Mlac-*hydro* and wild-type mice

Breed	Age (Day)	Sex	BUN (mg/dl)	Creatinine (mg/dl)	Urine specific gravity
ICR/Mlac-*hydro*	60	male	18.2 ± 2.49	0.125 ± 0.05	1.037 ± 0.013
Wild type	60	male	21.5 ± 2.41	0.133 ± 0.05	1.050 ± 0.000
p-value			0.137	0.846	0.164

cal software version 20. Statistical significance was defined as $P < 0.05$.

Results

Histomorphology

Microscopic analysis revealed that, the hydronephrotic kidneys exhibited dilation of the renal calyces, with a striking atrophy of the transitional epithelium of the renal pelvises and calyces (**Figure 1A**, **1B**). There was no evidence of interstitial fibrosis or glomerulosclerosis (**Figure 1D**). The percentage of renal parenchyma was significantly lower in ICR/Mlac-*hydro* mice compared to the wild-type (**Table 1**).

Clinical data

Clinical blood chemistry was compared between ICR/Mlac-*hydro* and wild-type mice. Similar to our previously work [15], levels of BUN, creatinine, and urine specific gravity in both strains of mice were identical (**Table 2**).

Comparative proteomics analysis

2DE was conducted to identify the differently expressed proteins between ICR/Mlac-*hydro* and wild-type mice. Three specimens of each group were analyzed at least three times to eliminate random error. Master 2D software from GE Healthcare® was used to automatically match the gels. The results exhibited a totally of 669 protein spots in which 131 protein spots had a significantly different expression. When compared to wild-type mice, 17 proteins were consistently up-regulated, 13 were consistently down-regulated, 50 were not expressed in ICR/Mlac-*hydro* mice, while 51 were not expressed in wild-type mice.

MS/MS analysis and protein identification

As shown in **Figure 2** and **Table 3**, 20 differentially expressed protein spots were selected and identified by MS analysis. The results showed that two sets of protein spots (spot number 9-10 and 16-17) were identical. Interestingly, among the identified proteins, 50.0% (9/18) were mitochondrial proteins which play roles in apoptosis and cell proliferation. In addition, 11.2% (2/18) were structural proteins related to the cytoskeletal system function. 22.3% (4/18) included enzymes and catalytic agents in the cytoplasm, and 16.6% (3/18) contained blood components.

Validation of altered proteins by immunohistochemistry

In order to validate the altered protein expression from the 2DE gel results and to exclude the experimental errors, immunohistochemical staining was performed on two chosen protein markers. This technique is an excellent detection to determine exactly where given proteins are located within the examined tissue. As shown in **Figure 3**, Hsp60 and Tubb4b were expressed in the cytoplasm of the collecting duct and apical membrane of distal tubule, respectively. The levels of their expression in ICR/Mlac-*hydro* were significantly higher than those of the wild-type, which were in good agreement with the 2DE gel results.

Discussion

Proteomic analysis on tissues, as an approach to investigate the pathophysiology of diseases, has achieved widespread acceptance in renal disease research [17-21]. Only a few proteins are known to be affected by hydronephrosis and the pathogenesis underlying this renal abnormality remains unclear. In this study, MS-based comparative proteomic analyses were applied to the kidneys of both ICR/Mlac-*hydro* and wild-type mice. Proteins with comparable expression levels were investigated, and their association with the pathogenesis of hydronephrosis was analyzed. As shown in **Table 3**, our study identified 20 stably, significantly altered proteins which functioned in multiple biological processes mainly related to mitochondrial proteins (Hsp60, GK, GRP75, VDAC-1, Dld, MCCase ∞, PCB, Sd, and IVD). We also identified some structural (cytoskeleton)

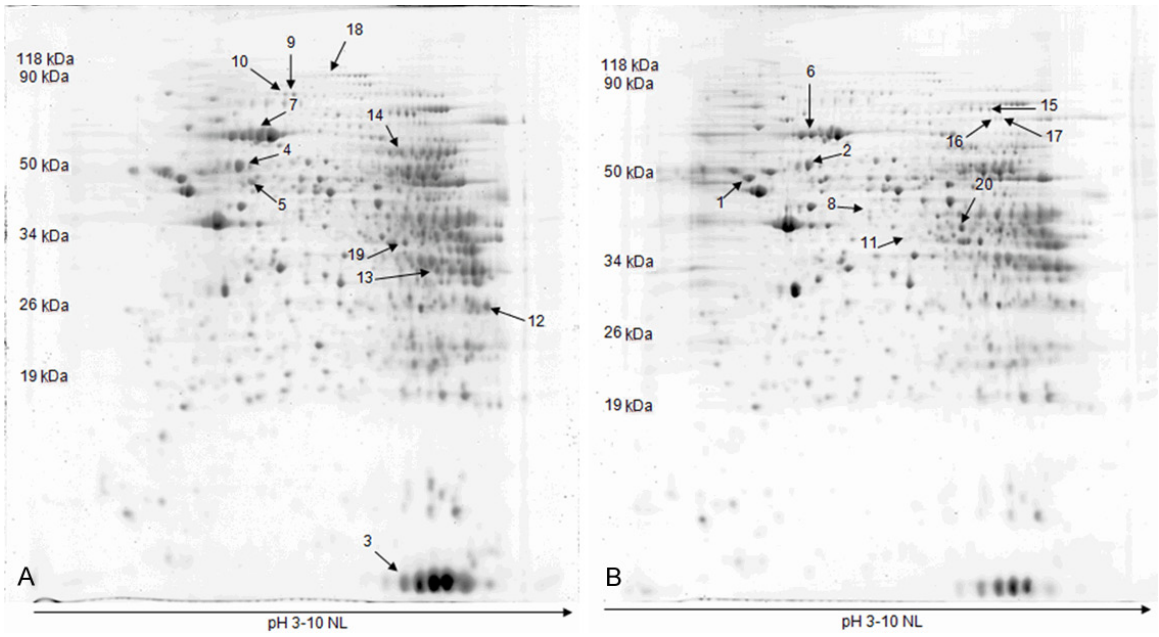

Figure 2. 2DE of ICR/Mlac-*hydro* mouse and wild-type mouse. Total protein extracts from ICR/Mlac-*hydro* mouse No. 2 (A) and wild-type mouse No. 1 (B) were separated on pH 3-10 IPG strips in the first dimension and followed by SDS-PAGE in the second dimension and visualized by Flamingo™ Fluorescent gel staining.

proteins (Tb4B and Ndr-1), some enzymes and cytoplasmic catalytic agents (Cnsd, V-ATPase A, 10-FTHFDH, and GAPDH), and a few blood components (Hb-b1, Alb, and Transferrin). To further validate these 2DE results, two selected proteins, Tb4B and Hsp60, from MS proteomics were confirmed by immunohistochemistry on renal tissues of both strains. These results showed similar up-regulation levels, thus confirming the proteomic data.

Biological activities of mitochondria are not only limit to the powerhouse of the cell, but also include biosynthetic pathways, calcium homeostasis, thermogenesis, cell death by apoptosis, and several different signal transduction pathways [25]. Indeed, a growing number of studies which assign a significant pathogenic role to damaged mitochondria in different diseases: ischemia/reperfusion injury [26], neurodegenerative diseases [27], metabolic syndrome, cardiovascular diseases, cancer [28], and hyperlipidemias [29]. Moreover, mitochondria dysfunction in the kidney plays a critical role in the pathogenesis of kidney diseases [30]. The renal manifestations that have been reported in relation to mitochondrial dysfunction include renal tubular dysfunction [31], interstitial nephritis, glomerular pathology [32], and in rare cases cystic disease [33]. There are two forms of renal manifestations in relation to mitochondrial dysfunction [34], with or without some well-recognized mitochondrial disease syndromes, such as Pearson syndrome, KearnsSayre syndrome, and Leigh syndrome.

Although there have been few reports regarding links between mitochondria dysfunction to hydronephrosis, Bushma's study demonstrated that in rabbits given gentamicin induced nephrotoxicity condition reduced the mitochondria's ability to oxidize alpha-ketoglutarate, palmitoilkarnitin, and succinate, predisposition to hydronephrosis [35]. To the best of our knowledge, our study reported here is the first to show a direct relationship between hydronephrosis and alterations of mitochondrial & cytoskeletal protein. However, the exact functional roles of these mitochondria-associated proteins in hydronephrosis need further study.

Hsp60 (60 kDa heat shock protein) and GRP75 (Stress-70 protein) are heat shock proteins and the most important chaperones found in the mitochondrial matrix [36]. Heat shock proteins act as protecting intracellular proteins from heat shock, toxicity, hypoxia, and inflammation

Table 3. Differently expressed proteins comparison between wild type and ICR/Mlac-*hydro* (the mutant) mice

Spot number	Intensity		ANOVA	Gene name	Protein name	Sequence coverage	Location	Function
	Wild type	Mutant						
1	0.4616	0.7988	0.0088	Tubb4b	Tubulin beta-4B chain (Tb4B)	59%	Microtubule	Chief component of microtubules [52]
2	0.5925	0.8195	0.0116	Hspd1	60 kDa heat shock protein (Hsp60)	73%	Mitochondria	Implicate in mitochondrial protein import and macromolecular assembly [36]
3	0.7653	0.0000	0.0064	Hbb-b1	Hemoglobin subunit beta-1 (Hb-b1)	77%	Red blood cell	Oxygen transportation
4	0.0712	0.1164	0.0063	Gk	Glycerol kinase (GK)	48%	Mitochondria	Enzyme in the regulation of glycerol uptake and metabolism [45]
5	0.1870	0.2667	0.0203	Cndp2	Cytosolic non-specific dipeptidase (Cnsd)	50%	Cytoplasm	Hydrolyze a variety of dipeptides including L-carnosine [65]
6	0.5128	0.6844	0.0030	Atp6v1a	V-type proton ATPase catalytic subunit A (V-ATPase A)	64%	Cytoplasm	Responsible for acidifying a variety of intracellular compartments in eukaryotic cells [59]
7	0.3490	0.0000	0.0000	HSPA9	Stress-70 protein (GRP75)	53%	Mitochondria	Implicate in the control of cell proliferation and cellular aging [37]
8	0.0163	0.0928	0.0371	Ndrg1	N-myc downstream-regulated gene 1 protein (Ndr 1)	22%	Microtubule	Chief component of microtubules [53]
9	0.0076	0.1018	0.0127	Aldh1l1	Cytosolic 10-formyltetrahydrofolate dehydrogenase (10-FTHFDH)	47%	Cytoplasm	Induce catalytic activity [66]
10	0.0406	0.0225	0.0148	Aldh1l1	Cytosolic 10-formyltetrahydrofolate dehydrogenase (10-FTHFDH)	36%	Cytoplasm	Induce catalytic activity [66]
11	0.0000	0.0738	0.0452	Alb	Serum albumin (Alb)	36%	Blood	Regulation of the colloidal osmotic pressure of blood
12	0.4130	0.0000	0.0032	Vdac1	Voltage-dependent anion-selective channel protein 1 (VDAC-1)	59%	Mitochondria	Responsible for the release of mitochondrial products that triggers apoptosis [42, 43]
13	0.5698	0.1479	0.0353	Gapdh	Glyceraldehyde-3-phosphate dehydrogenase (GAPDH)	34%	Cytoplasm	Play a role in glycolysis and nuclear functions [63]
14	0.1723	0.2155	0.0441	Dld	Dihydrolipoyl dehydrogenase (Dld)	35%	Mitochondria	Involve in the hyperactivation of spermatazoa during capacitation and in the spermatazoal acrosome reaction [46, 47]
15	0.0778	0.1693	0.0437	Tf	Serotransferrin (Transferrin)	62%	Blood	Responsible for the transport of iron
16	0.0320	0.0428	0.0228	Mccc1	Methylcrotonoyl-CoA carboxylase subunit alpha (MCCase ∞)	36%	Mitochondria	A critical enzyme for leucine and isovaleric acid catabolism [67]
17	0.0381	0.0621	0.0206	Mccc1	Methylcrotonoyl-CoA carboxylase subunit alpha (MCCase ∞)	21%	Mitochondria	A critical enzyme for leucine and isovaleric acid catabolism [67]
18	0.0000	0.0326	0.0056	Pc	Pyruvate carboxylase (PCB)	20%	Mitochondria	Catalyze initiates reactions of glucose and lipid synthesis from pyruvate [49]
19	0.3050	0.0220	0.0011	Sord	Sorbitol dehydrogenase (Sd)	57%	Mitochondria	Play an important role in sperm physiology [47]
20	0.3265	0.1065	0.0022	Ivd	Isovaleryl-CoA dehydrogenase (IVD)	50%	Mitochondria	Catalytic activity in mitochondria [51]

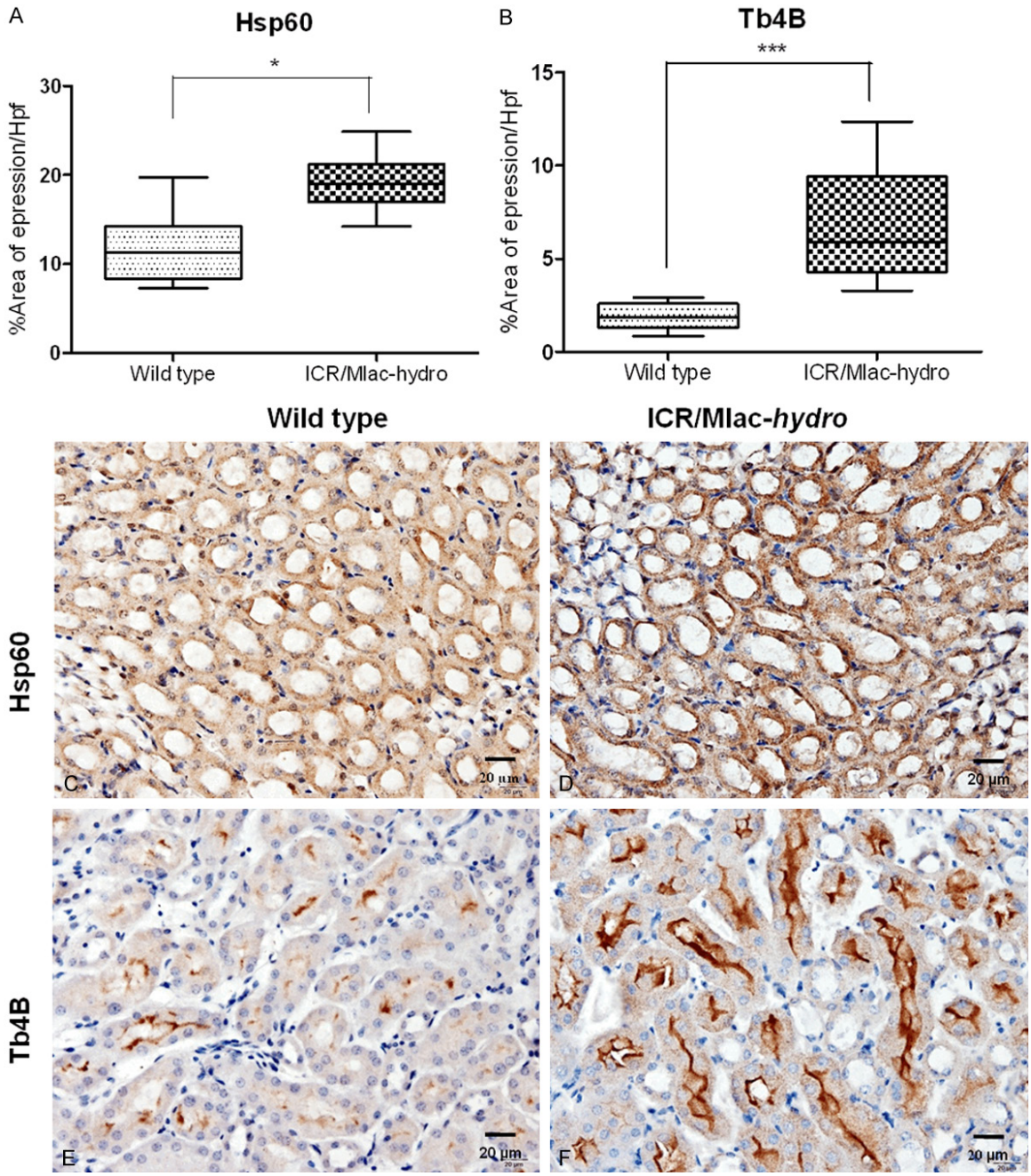

Figure 3. The expression of 60 kDa heat shock protein and Tubulin beta-4B chain in kidney. (A, B) Box plot demonstrates the difference of % area of expression/Hpf of Hsp60 and Tb4B in wild type compared to ICR/Mlac-*hydro* mouse. (C-F) Immunohistochemical staining of 60 days old male wild type (C&E) and ICR/Mlac-*hydro* (D&F) mouse kidney characterized Hsp60 localized in cytoplasm of collecting tubule (C&D) and Tb4B localized on apical membrane of distal tubule (E&F). *; *p*-value < 0.05, ***; *p*-value < 0.001.

[37]. GRP75 is also called mortalin which involved in stress response, cell proliferation, and apoptosis inhibition [38]. In case of cell damage and necrosis, heat shock proteins are released into circulation and play a protective role as danger signal [37, 39]. Chronic kidney disease alters the level of Hsp60 and GRP75, suggesting an adaptive response [40]. It has been found that increased expression of GRP75 in the cell results in a decreased tendency toward apoptosis [38, 41]. Our finding in the present study suggested that, the elevation

of Hsp60 in the ICR/Mlac-*hydro* mice may be associated with the stress conditions from urinary flow disturbance in hydronephrosis. While GRP75 was presented in wild-type mice, there was not found in ICR/Mlac-*hydro* mice. This refers that GRP75 dysfunction appears to have occurred in hydronephrotic condition probably resulting in high predisposition to cellular damage from apoptosis.

Voltage-dependent anion selective channel protein1 (VDAC-1) is located on the outer membrane of the mitochondria and helps form of the permeability transition pore complex (PTPC) responsible for the release of mitochondrial products that triggers apoptosis [42]. The reduction of VDAC-1 expression may be beneficial to synaptic activity, improve function, and protect against toxicities of Alzheimer's disease [43]. In accordance with other altered protein expressions in this study, reduced the level of VDAC-1 expression in ICR/Mlac-*hydro* mice may be related to an adaptive response to survive in the hydronephrotic condition since mutant mice can survive and maintain normal levels of renal enzymes for their entire lives [15].

It is noteworthy that, there are interaction among Hsp60, VDAC-1, and GRP75 [38]. GRP75 interacts with Hsp60 then promotes the entering of mitochondrial matrix compartment as the motor importer. This coupling process enhances the role of Hsp60 in proteins to refold, assembly, sort, and perform their corresponding function. GRP75 also interacts with VDAC-1 and modulates its channel properties. In ICR/Mlac-*hydro* mice, it is possible that GRP75 dysfunction may contribute to Hsp60 and VDAC-1 anomaly and involve in pathogenesis of hydronephrosis.

In humans, Glycerol kinase (GK) deficiency results in a wide range of phenotypic variability: severe metabolic problems, CNS abnormalities, hyperglycerolemia, and glyceroluria [44]. Mutant mice with X-linked GK deficiency show growth retardation, altered fat metabolism, autonomous glucocorticoid secretion, and neonatal death [45]. Dihydrolipoyl dehydrogenase (Dld) and sorbitol dehydrogenase (Sd) are also located in mitochondria, involve in the hyperactivation of spermatozoa [46] and sperm motility [47]. Methylcrotonoyl-CoA carboxylase subunit alpha (MCCase ∞) deficiency is inherited as an autosomal recessive trait resulting in clinical phenotype of seizures, muscular hypotonia, and aciduria [48]. Pyruvate carboxylase (PCB), located in mitochondrial matrix, is a catalyst that initiates reactions of glucose and lipid synthesis from pyruvate [49]. PCB deficiency has a complex form of lethal metabolic acidosis, renal tubular acidosis, hyperammonemia, and citrullinemia [50]. Isovaleryl-CoA dehydrogenase (IVD) deficiency in humans causes acidemia [51]. Although all described mitochondrial proteins are not directly associated with the pathophysiology of hydronephrosis, they are indicators for several kinds of mitochondrial protein alteration in ICR/Mlac-*hydro* mice.

Tubulin, present in all eukaryotes, is the chief component of microtubules (cytoskeleton) and consists of two similar but not identical subunits, ∞- and β-tubulin [52]. Like tubulin, N-myc downstream-regulated gene 1 protein (Ndr-1) is also located in the microtubule, and involved in regulating microtubule dynamics [53]. The cytoskeleton plays a fundamental role in maintaining cell morphology and tissue stability, as well as cellular motility, cell proliferation, and cell communication [54]. Several physiologic conditions have been linked to the disturbance of the cytoskeleton, including cardiovascular diseases, muscular degeneration, neurodegenerative diseases, cancers, cirrhosis, pulmonary fibrosis, and some skin diseases [55]. Disruption of primary cilium is associated with polycystic kidney disease, resulting from cilia loss with both altered microtubule stability and increased ∞-tubulin acetyl transferase activity [56]. Renal ischemia-reperfusion induced expression and redistribution of actin and microtubule cytoskeleton components in renal tubules is characterized by strongly increased actin and tubulin expressions [57]. In addition, Ndr-1 is involved in cystogenesis in polycystic kidney disease transgenic mouse model, exhibiting high level of Ndr-1 protein in the cyst lining epithelial [58]. In our study, Tubulin beta-4B chain (Tb4B) and Ndr-1 were up-regulated in the mutant mice. This suggests that hydronephrosis can induce changes in the renal cytoskeleton, Tb4B and Ndr-1, which react to an altered environment enhanced by a pressure-induced stretch of the renal tubular cells which can lead to tubular collapse and hypoxia.

Following the significantly altered proteins, some cytoplasmic enzymes and catalyzes were identified. V-type proton ATPase catalytic subunit A (V-ATPase A) is associated to luminal acidification in the kidney collecting duct and the epididymis/vas deference by vesicle recycling and transcytotic pathways [59]. Cytosolic non-specific dipeptidase (Cnsd) is linked to the risk of nephropathy in type 2 diabetes [60] and Parkinson's disease [61]. Cytosolic 10-formyltetrahydrofolate dehydrogenase (10-FTHFDH) is associated with folate deficiency due to alcohol intake [62]. These described proteins do not appear to be associated with congenital hydronephrosis. Glyceraldehyde-3-phosphate dehydrogenase (GAPDH) modulates and assemblies of the cytoskeleton [63] and a loss of glycolytic activity of GAPDH has been found in transgenic models and postmortem tissues of several neurodegenerative diseases [64]. Down-regulation of GAPDH in mutant mice may reduce the capacity of cytoskeleton modulation resulting in a dysfunction.

In summary, the renal proteome of ICR/Mlac-*hydro* mice significantly differs from the renal proteome of wild-type mice. Our study highlights some interesting proteins which may be involved in the pathogenesis of congenital hydronephrosis, not only through mitochondrial protein alteration but also accompanied by the alteration of structural proteins. This information may be used as a basis for further genomic studies to obtain more detailed descriptions of this strain as an animal model for the study of urinary tract diseases in biomedical research.

Acknowledgements

This research project was supported by Mahidol University, grant No. A28/2555, Faculty of Tropical Medicine and Department of Microbiology, Faculty of Science, Mahidol University. We are very grateful to project facilitator, Dr. Yaowaluk Panavechkijkul and Mrs. Malinee Tangluang, National Laboratory Animal Center, Mahidol University, who performed autopsy and managed project disbursement, respectively.

Disclosure of conflict of interest

None.

Address correspondence to: Dr. Sumate Ampawong, Department of Tropical Pathology, Faculty of Tropical Medicine, Mahidol University, 420/6, Ratchawithi Road, Ratchathewi, Bangkok 10400, Thailand. Tel: (662) 3549100-4 Ext. 1670; Fax: (662) 6447938; E-mail: am_sumate@hotmail.com

References

[1] Kumar V, Abbas AK and Aster JC. Roobbins' basic pathology. Philadelphia PA: Elesvier Saunders; 2013.

[2] Percy DH and Barthold SW. Pathology of laboratory rodents and rabbits. Ames: Iowa State University Press; 2007.

[3] McDill BW, Li SC, Kovach PA, Ding L and Chen F. Congenital progressive hydronephrosis (cph) is caused by an S256L mutation in aquaporin-2 that affects its phosphorylation and apical membrane accumulation. Proc Natl Acad Sci U S A 2006; 103: 6952-6957.

[4] Abdulaziz Kari J, Habiballah S, Alsaedi SA, Alsaggaf H, Al-dabbagh A, AbulHamail A, Marzouki A and Eldeek B. Incidence and outcomes of antenatally detected congenital hydronephrosis. Ann Saudi Med 2013; 33: 260-264.

[5] Kim MA, Yee NH, Choi JS, Choi JY and Seo K. Prevalence of birth defects in Korean livebirths, 2005-2006. J Korean Med Sci 2012; 27: 1233-1240.

[6] Sairam S, Al-Habib A, Sasson S and Thilaganathan B. Natural history of fetal hydronephrosis diagnosed on mid-trimester ultrasound. Ultrasound Obstet Gynecol 2001; 17: 191-196.

[7] Cohen BJ, De Bruin RW and Kort WJ. Heritable hydronephrosis in a mutant strain of brown Norway rats. Lab Anim Care 1970; 20: 489-493.

[8] Goto N, Nakajima Y, Onodera T and Imamura K. Inheritance of hydronephrosis in the inbred mouse strain DDD. Lab Anim 1984; 18: 22-25.

[9] Horton CE Jr, Davisson MT, Jacobs JB, Bernstein GT, Retik AB and Mandell J. Congenital progressive hydronephrosis in mice: a new recessive mutation. J Urol 1988; 140: 1310-1315.

[10] Nakajima Y, Imamura K, Onodera T, Motoi Y and Goto N. Hydronephrosis in the inbred mouse strain DDD. Lab Anim 1983; 17: 143-147.

[11] Takano K, Ogura A, Suzuki O, Noguchi Y, Yamamoto Y, Kurosawa S and Asano T. Hereditary hydronephrosis in C57L/MsNrs mice. Jikken Dobutsu 1993; 42: 107-109.

[12] Taylor DM and Fraser H. Hydronephrosis in inbred strains of mice with particular reference to the BRVR strain. Lab Anim 1973; 7: 229-236.

[13] Weide LG and Lacy PE. Hereditary hydronephrosis in C57BL/KsJ mice. Lab Anim Sci 1991; 41: 415-418.
[14] Kengkoom K, Zwa KM, Inpunkaew R, Angkhasirisap W, Thongsiri P and Ampawong S. Development of Hydronephrosis Inbred Strain Mouse, ICR/Mlac-Hydro. Journal of Animal and Veterinary Advances 2012; 11: 2054-2058.
[15] Ampawong S, Klincomhum A, Likitsuntonwong W, Singha O, Ketjareon T, Panavechkijkul Y, Zaw KM and Kengkoom K. Expression of aquaporin-1, -2 and -4 in mice with a spontaneous mutation leading to hydronephrosis. J Comp Pathol 2012; 146: 332-337.
[16] Suntornsaratoon P, Wongdee K, Tiyasatkulkovit W, Ampawong S, Krishnamra N, Kengkoom K and Charoenphandhu N. Defective Bone Microstructure in Hydronephrotic Mice: A Histomorphometric Study in ICR/Mlac-hydro Mice. Anat Rec (Hoboken) 2014; 297: 208-214.
[17] Frantzi M, Bitsika V, Charonis A and Vlahou A. Proteomics approaches in the quest of kidney disease biomarkers. Prilozi 2011; 32: 33-51.
[18] Wang G, Lai FM, Tam LS, Li KM, Lai KB, Chow KM, Li KT and Szeto CC. Messenger RNA expression of podocyte-associated molecules in urinary sediment of patients with lupus nephritis. J Rheumatol 2007; 34: 2358-2364.
[19] Kanno K, Kawachi H, Uchida Y, Hara M, Shimizu F and Uchiyama M. Urinary sediment podocalyxin in children with glomerular diseases. Nephron Clin Pract 2003; 95: c91-99.
[20] Ko GJ, Grigoryev DN, Linfert D, Jang HR, Watkins T, Cheadle C, Racusen L and Rabb H. Transcriptional analysis of kidneys during repair from AKI reveals possible roles for NGAL and KIM-1 as biomarkers of AKI-to-CKD transition. Am J Physiol Renal Physiol 2010; 298: F1472-1483.
[21] Decramer S, Zurbig P, Wittke S, Mischak H, Bascands JL and Schanstra JP. Identification of urinary biomarkers by proteomics in newborns: use in obstructive nephropathy. Contrib Nephrol 2008; 160: 127-141.
[22] Li QW, Lu XY, You Y, Sun H, Liu XY, Ai JZ, Tan RZ, Chen TL, Chen MZ, Wang HL, Wei YQ and Zhou Q. Comparative proteomic analysis suggests that mitochondria are involved in autosomal recessive polycystic kidney disease. Proteomics 2012; 12: 2556-2570.
[23] Shevchenko A, Wilm M, Vorm O and Mann M. Mass spectrometric sequencing of proteins silver-stained polyacrylamide gels. Anal Chem 1996; 68: 850-858.
[24] Ampawong S, Chaisri U, Viriyavejakul P, Nontprasert A, Grau GE and Pongponratn E. Electron microscopic features of brain edema in rodent cerebral malaria in relation to glial fibrillary acidic protein expression. Int J Clin Exp Pathol 2014; 7: 2056-2067.
[25] Scatena R. Advances in mitochondrial medicine. London: Springer, 2012.
[26] Silachev DN, Plotnikov EY, Pevzner IB, Zorova LD, Babenko VA, Zorov SD, Popkov VA, Jankauskas SS, Zinchenko VP, Sukhikh GT and Zorov DB. The Mitochondrion as a Key Regulator of Ischaemic Tolerance and Injury. Heart Lung Circ 2014; 23: 897-904.
[27] Hroudova J, Singh N and Fisar Z. Mitochondrial dysfunctions in neurodegenerative diseases: relevance to Alzheimer's disease. Biomed Res Int 2014; 2014: 175062.
[28] Sorriento D, Pascale AV, Finelli R, Carillo AL, Annunziata R, Trimarco B and Iaccarino G. Targeting mitochondria as therapeutic strategy for metabolic disorders. ScientificWorldJournal 2014; 2014: 604685.
[29] Alberici LC, Vercesi AE and Oliveira HC. Mitochondrial energy metabolism and redox responses to hypertriglyceridemia. J Bioenerg Biomembr 2011; 43: 19-23.
[30] Che R, Yuan Y, Huang S and Zhang A. Mitochondrial dysfunction in the pathophysiology of renal diseases. Am J Physiol Renal Physiol 2014; 306: F367-378.
[31] Saada A, Shaag A, Arnon S, Dolfin T, Miller C, Fuchs-Telem D, Lombes A and Elpeleg O. Antenatal mitochondrial disease caused by mitochondrial ribosomal protein (MRPS22) mutation. J Med Genet 2007; 44: 784-786.
[32] Gasser DL, Winkler CA, Peng M, An P, McKenzie LM, Kirk GD, Shi Y, Xie LX, Marbois BN, Clarke CF and Kopp JB. Focal segmental glomerulosclerosis is associated with a PDSS2 haplotype and, independently, with a decreased content of coenzyme Q10. Am J Physiol Renal Physiol 2013; 305: F1228-1238.
[33] Niaudet P and Rotig A. The kidney in mitochondrial cytopathies. Kidney Int 1997; 51: 1000-1007.
[34] O'Toole JF. Renal manifestations of genetic mitochondrial disease. Int J Nephrol Renovasc Dis 2014; 7: 57-67.
[35] Bushma KM. [The role of the functional state of kidney mitochondria in predisposition of hydronephrotic rabits to gentamicin nephrotoxicity]. Eksp Klin Farmakol 2008; 71: 26-30.
[36] Voos W and Röttgers K. Molecular chaperones as essential mediators of mitochondrial biogenesis. Biochim Biophys Acta 2002; 1592: 51-62.
[37] Gabai VL and Sherman MY. Invited review: Interplay between molecular chaperones and signaling pathways in survival of heat shock. J Appl Physiol 2002; 92: 1743-1748.

[38] Londono C, Osorio C, Gama V and Alzate O. Mortalin, apoptosis, and neurodegeneration. Biomolecules 2012; 2: 143-164.
[39] Osterloh A and Breloer M. Heat shock proteins: linking danger and pathogen recognition. Med Microbiol Immunol 2008; 197: 1-8.
[40] Musial K, Szprynger K, Szczepanska M and Zwolinska D. The heat shock protein profile in children with chronic kidney disease. Perit Dial Int 2010; 30: 227-232.
[41] Ravagnan L, Gurbuxani S, Susin SA, Maisse C, Daugas E, Zamzami N, Mak T, Jaattela M, Penninger JM, Garrido C and Kroemer G. Heat-shock protein 70 antagonizes apoptosis-inducing factor. Nat Cell Biol 2001; 3: 839-843.
[42] Sampson MJ, Lovell RS and Craigen WJ. Isolation, characterization, and mapping of two mouse mitochondrial voltage-dependent anion channel isoforms. Genomics 1996; 33: 283-288.
[43] Manczak M, Sheiko T, Craigen WJ and Reddy PH. Reduced VDAC1 protects against Alzheimer's disease, mitochondria, and synaptic deficiencies. J Alzheimers Dis 2013; 37: 679-690.
[44] Wightman PJ, Jackson GR and Dipple KM. Glycerol hypersensitivity in a Drosophila model for glycerol kinase deficiency is affected by mutations in eye pigmentation genes. PLoS One 2012; 7: e31779.
[45] Huq AH, Lovell RS, Ou CN, Beaudet AL and Craigen WJ. X-linked glycerol kinase deficiency in the mouse leads to growth retardation, altered fat metabolism, autonomous glucocorticoid secretion and neonatal death. Hum Mol Genet 1997; 6: 1803-1809.
[46] Johnson M, Yang HS, Johanning GL and Patel MS. Characterization of the mouse dihydrolipoamide dehydrogenase (Dld) gene: genomic structure, promoter sequence, and chromosomal localization. Genomics 1997; 41: 320-326.
[47] Cao W, Aghajanian HK, Haig-Ladewig LA and Gerton GL. Sorbitol can fuel mouse sperm motility and protein tyrosine phosphorylation via sorbitol dehydrogenase. Biol Reprod 2009; 80: 124-133.
[48] Bannwart C, Wermuth B, Baumgartner R, Suormala T and Weismann UN. Isolated biotin-resistant deficiency of 3-methylcrotonyl-CoA carboxylase presenting as a clinically severe form in a newborn with fatal outcome. J Inherit Metab Dis 1992; 15: 863-868.
[49] Rardin MJ, Newman JC, Held JM, Cusack MP, Sorensen DJ, Li B, Schilling B, Mooney SD, Kahn CR, Verdin E and Gibson BW. Label-free quantitative proteomics of the lysine acetylome in mitochondria identifies substrates of SIRT3 in metabolic pathways. Proc Natl Acad Sci U S A 2013; 110: 6601-6606.
[50] Nyhan WL, Khanna A, Barshop BA, Naviaux RK, Precht AF, Lavine JE, Hart MA, Hainline BE, Wappner RS, Nichols S and Haas RH. Pyruvate carboxylase deficiency--insights from liver transplantation. Mol Genet Metab 2002; 77: 143-149.
[51] Willard JM, Reinard T, Mohsen A and Vockley J. Cloning of genomic and cDNA for mouse isovaleryl-CoA dehydrogenase (IVD) and evolutionary comparison to other known IVDs. Gene 2001; 270: 253-257.
[52] Wolff J. Plasma membrane tubulin. Biochim Biophys Acta 2009; 1788: 1415-1433.
[53] Okuda T, Higashi Y, Kokame K, Tanaka C, Kondoh H and Miyata T. Ndrg1-deficient mice exhibit a progressive demyelinating disorder of peripheral nerves. Mol Cell Biol 2004; 24: 3949-3956.
[54] Fuchs E and Cleveland DW. A structural scaffolding of intermediate filaments in health and disease. Science 1998; 279: 514-519.
[55] Ramaekers FC and Bosman FT. The cytoskeleton and disease. J Pathol 2004; 204: 351-354.
[56] Berbari NF, Sharma N, Malarkey EB, Pieczynski JN, Boddu R, Gaertig J, Guay-Woodford L and Yoder BK. Microtubule modifications and stability are altered by cilia perturbation and in cystic kidney disease. Cytoskeleton (Hoboken) 2013; 70: 24-31.
[57] Caron A, Desrosiers RR and Beliveau R. Kidney ischemia-reperfusion regulates expression and distribution of tubulin subunits, beta-actin and rho GTPases in proximal tubules. Arch Biochem Biophys 2004; 431: 31-46.
[58] Kim BH, Park EY, Yoo KH, Choi KM, Kim Y, Seong J and Park JH. N-myc downstream-regulated gene 1 is involved in the regulation of cystogenesis in transgenic mice overexpressing human PKD2 gene. Proteomics 2013; 13: 134-141.
[59] Brown D and Breton S. H(+)V-ATPase-dependent luminal acidification in the kidney collecting duct and the epididymis/vas deferens: vesicle recycling and transcytotic pathways. J Exp Biol 2000; 203: 137-145.
[60] Ahluwalia TS, Lindholm E and Groop LC. Common variants in CNDP1 and CNDP2, and risk of nephropathy in type 2 diabetes. Diabetologia 2011; 54: 2295-2302.
[61] Licker V, Cote M, Lobrinus JA, Rodrigo N, Kovari E, Hochstrasser DF, Turck N, Sanchez JC and Burkhard PR. Proteomic profiling of the substantia nigra demonstrates CNDP2 overexpression in Parkinson's disease. J Proteomics 2012; 75: 4656-4667.
[62] Min H, Im ES, Seo JS, Mun JA and Burri BJ. Effects of chronic ethanol ingestion and folate deficiency on the activity of 10-formyltetrahy-

drofolate dehydrogenase in rat liver. Alcohol Clin Exp Res 2005; 29: 2188-2193.
[63] Arif A, Chatterjee P, Moodt RA and Fox PL. Heterotrimeric GAIT complex drives transcript-selective translation inhibition in murine macrophages. Mol Cell Biol 2012; 32: 5046-5055.
[64] Chuang DM, Hough C and Senatorov VV. Glyceraldehyde-3-phosphate dehydrogenase, apoptosis, and neurodegenerative diseases. Annu Rev Pharmacol Toxicol 2005; 45: 269-290.
[65] Otani H, Okumura N, Hashida-Okumura A and Nagai K. Identification and characterization of a mouse dipeptidase that hydrolyzes L-carnosine. J Biochem 2005; 137: 167-175.
[66] Park J, Chen Y, Tishkoff DX, Peng C, Tan M, Dai L, Xie Z, Zhang Y, Zwaans BM, Skinner ME, Lombard DB and Zhao Y. SIRT5-mediated lysine desuccinylation impacts diverse metabolic pathways. Mol Cell 2013; 50: 919-930.
[67] Baumgartner MR, Almashanu S, Suormala T, Obie C, Cole RN, Packman S, Baumgartner ER and Valle D. The molecular basis of human 3-methylcrotonyl-CoA carboxylase deficiency. J Clin Invest 2001; 107: 495-504.